analytical chemistry

Article

pubs.acs.org/ac

Ultrasound Characterization of Microbead and Cell Suspensions by Speed of Sound Measurements of Neutrally Buoyant Samples

Kevin W. Cushing,*[,†,⊥] Fabio Garofalo,*[,†,⊥] Cecilia Magnusson,[‡] Lars Ekblad,[§] Henrik Bruus,[∥] and Thomas Laurell[†]

[†]Department of Biomedical Engineering, Lund University, 221 00 Lund, Sweden

[‡]Department of Translational Medicine, Lund University, 221 00 Lund, Sweden

[§]Division of Oncology, Clinical Sciences, Lund University and Skane University Hospital, 221 00 Lund, Sweden

[∥]Department of Physics, Technical University of Denmark, 2800 Kongens Lyngby, Denmark

ABSTRACT: We present an experimental method including error analysis for the measurement of the density and compressibility of cells and microbeads; these being the two central material properties in ultrasound-based acoustophoretic applications such as particle separation, trapping, and up-concentration. The density of the microparticles is determined by using a neutrally buoyant selection process that involves centrifuging of microparticles suspended in different density solutions, CsCl for microbeads and Percoll for cells. The speed of sound at 3 MHz in the neutrally buoyant suspensions is measured as a function of the microparticle volume fraction, and from this the compressibility of the microparticles is inferred. Finally, from the obtained compressibility and density, the acoustic scattering coefficients and contrast factor of the microparticles are determined, and in a sensitivity analysis, the impact of the measurement errors on the computed acoustic properties is reported. The determination of these parameters and their uncertainties allow for accurate predictions of the acoustophoretic response of the microparticles. The method is validated by determining the density (0.1−1% relative uncertainty) and compressibility (1−3% relative uncertainty) of previously well-characterized polymer microbeads and subsequently applied to determine the density (0.1−1% relative uncertainty), compressibility (1% relative uncertainty), scattering coefficients, and acoustic contrast factors for nonfixed and fixed cells, such as red blood cells, white blood cells, DU-145 prostate cancer cells, MCF-7 breast cancer cells, and LU-HNSCC-25 head and neck squamous carcinoma cells in phosphate buffered saline. The results show agreement with published data obtained by other methods.

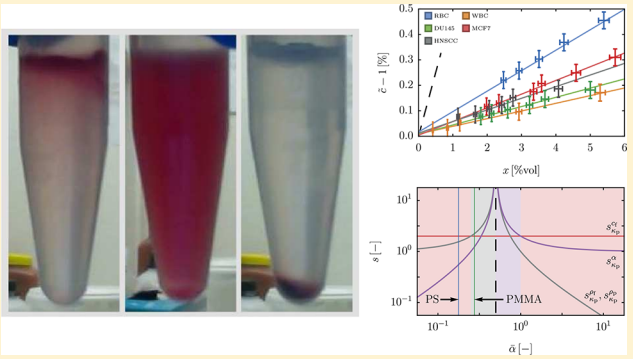

Acoustophoresis is a well-established technology to spatially manipulate microbeads and biological cells at the microscale. Indeed, it has been demonstrated that the combined action of acoustic pressure waves and a carrier fluid in an embedded microfluidic channel can be used for concentration,[1] trapping,[2] washing,[3] alignment, and separation of different cell types[4−7] with high accuracy and precision. The ability to isolate, separate, and enrich different cell types from biological matrixes, e.g., human blood, urine, cerebral spinal fluid, is important for clinical studies, such as cell differentiation, phenotype profiling, and determining the disease states of cells.[8−12]

The separation principle is based on the acoustic radiation force acting on a specific microparticle type. The acoustic radiation force depends on the ratio of the density and compressibility of the suspended microparticles and the surrounding medium as well as the frequency and energy density of the imposed ultrasound field.[13] The resulting migration, called acoustophoresis, can be used to separate microparticles with different acoustic properties, such as WBCs and cancerous cells.[5] The determination of the acoustic properties is a necessary prerequisite to predict and characterize any acoustophoretic handling of suspended microparticles.

Various techniques have been used to determine the mechanical properties of single cells, such as atomic force microscopy, optical tweezers, and glass micropipetting.[14−22] Specifically, the acoustophoretic mobility coefficient and the expression for the acoustic contrast factor have been employed together with microparticle tracking experiments to estimate the compressibility of microbeads and cells.[23] In these methods, the density and the radius of the microparticles were based on previously reported values and not derived within the experiments, thereby introducing uncertainties in the estimate of the measured quantities. Furthermore, this assumes that a population of cells can be characterized by single or a few

Received: April 13, 2017
Accepted: July 27, 2017
Published: July 27, 2017

ACS Publications © 2017 American Chemical Society

DOI: 10.1021/acs.analchem.7b01388
Anal. Chem. 2017, 89, 8917−8923

density, compressibility, and radius values, not truly representing the average properties of an entire cell population.

Recently, starting from measurements on the average particle radius and density, a microparticle tracking method was used to measure the compressibility of microbeads.[24] This microparticle tracking method used traveling acoustic waves where all acoustophoretic parameters were calibrated based on polystyrene values (density and compressibility) from reports[25] and were not derived within the experiment, thus leading to uncertainties in the measured quantities. Additionally, the microparticle tracking method tracks the position of single microbeads which is still on the single particle level and does not give population based data.

Average compressibility values of microparticle populations can be obtained from Wood's equation[26] by measuring the speed of sound in microparticle suspensions as a function of the microparticle concentration. Such measurements have been previously used to determine the compressibility of polystyrene microbeads and red blood cells (RBCs).[27,28] However, the density was not determined on the same samples but instead based on values reported in the literature, and the impact of the uncertainties of the measurement of the density, speed of sound and compressibility, was not addressed. Furthermore, the speed-of-sound measurements were not based on neutrally buoyant suspensions, which increase the measurement uncertainty due to combined dependence of density and compressibility as well as particle sedimentation, which occurs on the same time scale as the measurement process.

To determine the compressibility independently from the density, we perform the speed-of-sound measurements on neutrally buoyant suspensions. In this case, the speed of sound of the microparticle suspensions depends only on the volume fraction of the microparticles and on the compressibility of the microparticles relative to that of the fluid. This simplifies the determination of the parameters considerably without introducing additional difficulties in the experiments. The present paper describes not only the experimental method for the measurement of the density and the compressibility, but it also addresses a thorough analysis of the experimental errors that such a method introduces into the measured and derived quantities. Finally, from the density and compressibility it is possible to determine the acoustic scattering coefficients and the contrast factors of the microbeads and cell populations in specific suspension media and to assess the errors affecting the average measured values.

The neutrally buoyant ultrasound-based method we propose represents an improvement in measuring average acoustic properties by decoupling the measurement of the compressibility from the density.

THEORY REVIEW

Acoustophoretic Parameters. Consider a single microparticle of density ρ_p and compressibility κ_p suspended in a fluid with density ρ_f and compressibility κ_f. The acoustic monopole and dipole scattering coefficients are, respectively,

$$f_0(\tilde{\kappa}) = 1 - \tilde{\kappa} \tag{1}$$

$$f_1(\tilde{\rho}) = \frac{2(\tilde{\rho} - 1)}{2\tilde{\rho} + 1} \tag{2}$$

where $\tilde{\kappa} = \kappa_p/\kappa_f$ is the particle/fluid compressibility ratio and $\tilde{\rho} = \rho_p/\rho_f$ is the particle/fluid density ratio.

The acoustophoretic force $\boldsymbol{F}_{ac}$ on a microparticle of radius a is given by these scattering coefficients together with the acoustic pressure field p and velocity field v at the position of the particle.[13] For the special case of a standing plane wave in the z-direction $\hat{e}_z$, the force expression simplifies to

$$\boldsymbol{F}_{ac} = \frac{4\pi a^3}{3}\Phi_0(\tilde{\kappa}, \tilde{\rho})kE_{ac}\sin(2kz)\hat{e}_z \tag{3}$$

$$\Phi_0(\tilde{\kappa}, \tilde{\rho}) = f_0(\tilde{\kappa}) + \frac{3}{2}f_1(\tilde{\rho}) \tag{4}$$

where k is the acoustic wavenumber, E_{ac} is the acoustic energy density, and Φ_0 is the contrast factor. Consequently, the density and the compressibility of a microparticle are central in determining the acoustophoretic performance. Equations 1−4 have been used as main tools for the acoustophoretic determination of the acoustic energy density and the density and compressibility of cells.[29,30] In the present context, eqs 1, 2, and 4 will be used to compute the scattering coefficients, the contrast factors, and their errors.

Speed of Sound of Suspensions. The speed of sound in a fluid changes from c_f to c_s as microparticles are suspended in it with a volume fraction x. The relative speed of sound $\tilde{c} = c_s/c_f$ is given by the Wood's equation,[26,27] $\tilde{c} = [1 - (1 + \tilde{\kappa})\,x][1 - (1 + \tilde{\rho})\,x]^{-1/2}$. For $x \ll 1$, this expression reduces to a linear function of x

$$\tilde{c} = \alpha(\tilde{\kappa}, \tilde{\rho})x + 1, \quad x \ll 1 \tag{5}$$

$$\alpha(\tilde{\kappa}, \tilde{\rho}) = \frac{1}{2}[(1 - \tilde{\kappa}) + (1 - \tilde{\rho})] \tag{6}$$

At neutral buoyancy, the microparticle and the fluid densities are identical, so $\tilde{\rho} = 1$, and the slope α reduces to

$$\alpha(\tilde{\kappa}, 1) = \frac{1}{2}[(1 - \tilde{\kappa})], \quad \tilde{\rho} = 1 \tag{7}$$

in which case $f_0 = 2\,\alpha$, $\tilde{\kappa} = 1 - 2\alpha$, and the microparticle compressibility becomes $\kappa_p = (1 - 2\alpha)\kappa_f$.

Measurements and Errors. We consider n independent variables m_i, which by independent measurements is found to have averages $\bar{m}_i = \langle m_i \rangle$, variances $\sigma_i^2 = \langle (m_i - \bar{m}_i)^2 \rangle$, and relative errors $\epsilon_i = \sigma_i/\bar{m}_i$. The relative error ϵ_g on a quantity $g(m_1,...,m_n)$, which is a function of the measured variables, is given by the usual expression for the propagation of error, $\epsilon_g^2 = \sum_i [s_g^i(m_1, ..., m_n)]^2\,\epsilon_i^2$, where the sensitivity factors are given by $s_g^i(m_1, ..., m_n) = \left|\frac{\partial g}{\partial m_i}\bar{m}_i/\bar{g}\right|$ with $\bar{g} = \langle g(m_1,...,m_n)\rangle$. Details about the values of the errors and the relative errors are described in Methods.

For the fluid, the compressibility κ_f and the sensitivity factors are determined by the measured density $\bar{\rho}_f$ and the speed of sound $\bar{c}_f$

$$\bar{\kappa}_f = \frac{1}{\bar{\rho}_f\,\bar{c}_f{}^2}, \quad s_{\kappa_f}^{c_f} = 2, \quad s_{\kappa_f}^{\rho_f} = 1 \tag{8}$$

For the microparticle, the compressibility value $\bar{\kappa}_f$ can be calculated as

$$\bar{\kappa}_p = \bar{\kappa}_f\left[1 - 2\bar{\alpha} + \left(1 - \frac{\bar{\rho}_p}{\bar{\rho}_f}\right)\right] \tag{9}$$

with the corresponding sensitivity factors for the particle compressibility

DOI: 10.1021/acs.analchem.7b01388
Anal. Chem. 2017, 89, 8917−8923

$$s_{\kappa_p}^{c_f} = 2 \tag{10}$$

$$s_{\kappa_p}^{\rho_f} = s_{\kappa_p}^{\rho_p} = \frac{1}{(1 - 2\bar{\alpha})} \tag{11}$$

$$s_{\kappa_p}^{\alpha} = \frac{2\bar{\alpha}}{(1 - 2\bar{\alpha})} \tag{12}$$

Note that if $\alpha \approx 1/2$, three of the four sensitivity factors diverge. It is important to emphasize that if the microparticle compressibility approaches the compressibility of the fluid, the average slope $\bar{\alpha}$ approaches the value 1/2, and three of the four sensitivity factors diverge. In this case the measurements of $\bar{\kappa}_p$ becomes highly uncertain.

The measurements for the scattering coefficients are given by the averaged version of eqs 1 and 2) with $\tilde{\rho} = \bar{\rho}_p/\bar{\rho}_f$ and $\tilde{\kappa} = \bar{\kappa}_p/\bar{\kappa}_f$, and the corresponding sensitivity factors become

$$s_{f_0}^{\kappa_f} = s_{f_0}^{\kappa_p} = \frac{\bar{\kappa}_p/\bar{\kappa}_f}{\bar{f}_0} \tag{13}$$

$$s_{f_1}^{\rho_f} = s_{f_0}^{\rho_p} = \frac{6\bar{\rho}_p/\bar{\rho}_f}{\bar{f}_1\,(2\bar{\rho}_p/\bar{\rho}_f + 1)^2} \tag{14}$$

Finally, the acoustophoretic contrast factor $\bar{\Phi}_0$ follows from eq 4, again using $\tilde{\rho} = \bar{\rho}_p/\bar{\rho}_f$ and $\tilde{\kappa} = \bar{\kappa}_p/\bar{\kappa}_f$, and the sensitivity factors for Φ_0 are given by

$$s_{\Phi_0}^{\kappa_p} = s_{\Phi_0}^{\kappa_f} = \frac{\bar{\kappa}_p/\bar{\kappa}_f}{\bar{\Phi}_0} \tag{15}$$

$$s_{\Phi_0}^{\rho_p} = s_{\Phi_0}^{\rho_f} = \frac{9\bar{\rho}_p/\bar{\rho}_f}{\bar{\Phi}_0(2\bar{\rho}_p/\bar{\rho}_f + 1)^2} \tag{16}$$

METHODS

Density Measurements. *Suspensions and Solutions.* The densities of the suspensions and the density solutions reported in this work was measured using the density and speed of sound metering instrument DSA 5000 M (Anton Paar, Malmö, Sweden), for which the instrumental error is $\sigma_\rho^{DSA} \approx 10^{-2}$ kg/m^3.[31] The error for the density measurements σ_ρ ($\rho = \rho_f$ or ρ_s) is the root-sum-squared of the instrumental error $\sigma_{\rho f}^{DSA}$ and the standard deviation on the measurement set,

$$\sigma_\rho = \sqrt{(\sigma_\rho^{DSA})^2 + \langle(\rho - \bar{\rho})^2\rangle}, \quad \rho = \rho_f \text{ or } \rho_s \tag{17}$$

All the measurements in this work were carried out at T = 25 °C.

Microbeads. The material and diameter $2a$ of the polymer microbeads used in the validation were polystyrene $2a$ = 5 μm (PS5) and $2a$ = 7 μm (PS7), melamine $2a$ = 10 μm (MA), and poly(methyl methacrylate) $2a$ = 3 μm (PMMA), all from Sigma-Aldrich (Stockholm, Sweden). Their densities were determined using the following neutral-buoyancy selection process.

The microbeads were centrifugally washed in 1 mL of Milli-Q water with approximately 0.1%w (weight fraction) Pluronic F-108 surfactant (Sigma-Aldrich) at 3000g for 2 min. Solutions of different density were prepared by adding cesium chloride (CsCl, Sigma-Aldrich) to 0.1% w Pluronic F-108 in Milli-Q water, and their densities were measured. Microbeads were then added to each density solution and centrifuged at g_{cent} = 3000g for t_{cent} = 5 min. By visual inspection of the centrifugation results, the neutrally buoyant particle suspension was selected, its density ρ_s was measured, and the particle density was subsequently assigned that value, $\rho_p = \rho_s$. In this procedure, small deviations between the measured density ρ_f of the solution that made the particle neutrally buoyant and the particle (or suspension) density ρ_p were observed. To verify that microbead suspensions were neutrally buoyant, we doubled the centrifugation time (10 min), which gave us the same results in the neutrally buoyant solutions.

The error $\sigma_{\rho p}$ for the particle density $\bar{\rho}_p$ arises from the visual selection of the neutrally buoyant suspension. An upper bound on the particle density error $\sigma_{\rho p}$ is therefore obtained by using the centrifugation time t_{cent} as a lower bound of the time it takes a nearly neutral buoyant particle of density $\bar{\rho}_p = (1 + \epsilon_{\rho p})\,\bar{\rho}_f$, where $\epsilon_{\rho p} = \sigma_{\rho p}/\bar{\rho}_p$, to sediment/float for $H \approx 1$ cm (maximum-allowed vertical displacement) from the top/bottom of the vial at its terminal speed in the solution of density $\bar{\rho}_f$ and viscosity $\eta_f \simeq 1$ mPa s,

$$\sigma_{\rho_p} = \frac{9H\eta_w}{2g_{cent}\bar{a}^2 t_{cent}} \tag{18}$$

It has been observed experimentally that the error computed from eq 18 is larger than the error for the suspension density ρ_s given by the measurements through eq 17. In eq 18, the radii of the polymer beads and the cell populations were estimated by averaging Coulter Counter data (Multi-Sizer).

Cells. The density of cells was measured in the same way as that of microbeads but using a less intense centrifugation at g_{cent} = 200g to maintain the cell viability. Fixed and nonfixed populations of human RBC and WBC (RBC-lysed blood), along with various cultured cell lines, i.e., DU-145 (prostate cancer), MCF-7 (breast cancer), and LU-HNSCC-25 (head and neck squamous carcinoma), were added in phosphate buffered saline solutions (PBS, Sigma-Aldrich) at pH = 7.4 and centrifuged for 5 min at 200g. To allow visual inspection of the neutral buoyancy selection process, enough cells were added to the PBS solutions to make them opaque prior to centrifugation. The supernatant of the cell suspensions was then removed and the cells were resuspended in solutions of known densities. These density solutions were prepared by adding various amounts of Percoll into aqueous solutions (Milli-Q water) containing enough NaCl (Sigma-Aldrich) to make the solution isotonic with an osmolality between 300−340 mOsm/kg H_2O as to match the human serum range of osmolality (240−340 mOsm/kg H_2O), and the pH was adjusted to 7.4 by adding HCl (0.1 N). The cells were then resuspended in the density solutions and centrifuged at g_{cent} = 200g for t_{cent} = 5 min. The neutrally buoyant suspension was selected by visual inspection, its density was measured and taken to be the cell density. Also in this case small deviations between the density solution ρ_f and the cell density ρ_p were observed. Again, to verify that cell suspensions were neutrally buoyant, we doubled the centrifugation time (10 min), which gave us the same results in the neutrally buoyant solutions.

Particle Size and Volume Fraction. The volume fraction of microbeads and cells $x = \frac{N\frac{4}{3}\pi a^3}{V_f + N\frac{4}{3}\pi a^3}$ of particles in a given suspension of volume V_f were obtained by dilution of the neutrally buoyant microparticle suspensions into a known amount of the corresponding density matched solution. After dilution, the obtained volume fractions were measured using a

DOI: 10.1021/acs.analchem.7b01388
Anal. Chem. 2017, 89, 8917−8923

Coulter Counter (Multi-Sizer). The relative error for the volume fraction was computed from the relative error on the microparticle radius σ_a, that was estimated by measuring reference 20 μm polystyrene beads before and after the Coulter Counter calibration and considering the error as the difference between the before-calibration average radius and the after-calibration average radius. The relative error resulted to be $\epsilon_a \approx 10^{-2}$. By considering that for small particle volume fraction $x \simeq \frac{N\frac{4}{3}\pi a^3}{V_f}$ and having thus $s_x^a = 3$, the relative error on x is $\epsilon_x \approx 3 \times \epsilon_a = 3 \times 10^{-2}$.

Speed of Sound Measurements. For each neutrally buoyant particle suspension sample obtained after centrifugation, both the speed of sound c_s of that suspension and the speed of sound c_f of the corresponding density solution were measured at 3 MHz using a 2.5 mL sample volume in the density and speed of sound metering instrument DSA 5000M. The error σ_c ($c = c_f$ or c_s) for the speed of sound is the root-sum-squared of the instrumental error $\sigma_c^{DSA} \approx 0.5$ m/s[31] and the standard deviation of the measurement set

$$\sigma_c = \sqrt{(\sigma_c^{DSA})^2 + \langle (c - \bar{c})^2 \rangle}, \quad c = c_f \quad \text{or } c_s \tag{19}$$

For each type of particle, five to seven suspensions with different particle volume fractions were made, and their respective speed of sound were measured. The slope $\bar{\alpha}$ and its error σ_α were determined by orthogonal least-squares fitting[32] of the linear model eq 5, as to take into account for the errors on the volume fraction. The validation for the speed of sound measurements was performed by measuring the speed of sound in water at $T = 25$ °C that resulted in $c_f = 1496.9(5)$ m/s which is in accordance, within the given uncertainty, with the reference values.[33,34]

Cultured Cells and Blood Processing. Human cancer cell lines, DU-145 (prostate cancer) and MCF-7 (breast cancer), were acquired from the American Type Culture Collection (ATCC) and grown according to ATTC endorsed methods.[5] The head and neck squamous carcinoma cell line LU-HNSCC-25 was established in our laboratory and grown in Dulbecco's modified Eagle's medium supplemented with 10% fetal bovine serum, 100 units/mL penicillin, and 100 units/mL streptomycin sulfate. The concentrate of human blood and WBCs was furnished from the Lund University Hospital, (Lund, Sweden) from anonymous healthy donor volunteers. Blood vacutainer tubes containing ethylenediaminetetraacetic acid (EDTA) as an anticoagulant were used to obtain human blood samples. For experiments with RBC-lysed samples, the blood was lysed (without fixative) at room temperature for 15 min using BD Pharm Lyse solution (BD Bioscience), following BD approved methods.[5] Cell fixations (except RBC samples) were performed by incubation in PBS with 2% paraformaldehyde (PFA) for 15 min on ice.[5] Fixed cell samples were then centrifugally washed 2× with PBS at 200 for 5 min; fixed cell samples were then resuspended in PBS. Following the BD Biosciences approved method, RBC samples were fixed by incubation in cold PBS with 0.05% glutaraldehyde for 10 min. Fixed RBC samples were then centrifugally washed 2× with PBS at 200g for 5 min and resuspended in PBS.

RESULTS AND DISCUSSION

In this section, we (i) validate the method by performing density and compressibility measurements of polymer microbeads, (ii) apply the method to different cell populations that are commonly encountered in acoustophoretic applications, and (iii) use the derived density and compressibility to calculate the scattering coefficients and the acoustophoretic contrast factor for the different cell populations. An example of the neutral-buoyancy selection process for determination of the microparticle density is illustrated in Figure 1 for RBCs in three

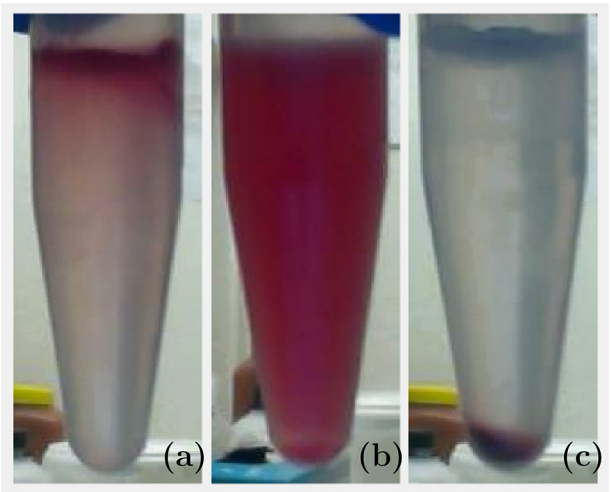

Figure 1. Visual example of the results after the centrifugation of three RBC suspensions with (a) positive buoyancy, (b) neutral buoyancy, and (c) negative buoyancy.

Percoll solutions of different densities corresponding to (a) positive, RBCs float over a denser solution, (b) neutral, RBCs equally dispersed in a solution with density $\rho_f = 1107.05$ kg/m^3, and (c) negative, RBCs sediment.

Method Validation. To validate the method, we measured the acoustic properties of polymer microbeads. Figure 2 shows the linear change in the relative speed of sound $\tilde{c} - 1$ for neutrally buoyant microbead suspensions as a function of the particle volume fraction x. The lines are obtained by fitting eq 5 to the experimental data (error crosses). Table 1 shows the numerical values obtained from the experimental analysis. In the case of neutrally buoyant suspensions, the slope increases as the compressibility ratio $\tilde{\kappa}$ decreases, see eq 7, so the largest and smallest slope is obtained for MA and PS7 microbeads, respectively. Polystyrene microbeads with different size were measured to demonstrate that the measurements of density and compressibility are weakly affected by the particle size in the method we propose. Although the particle diameters differ by 40%, the measured density and compressibility of the particle types differ less than 0.1% (see Table 1).

The sensitivity of the method is now discussed with the aid Figure 2b where the sensitivity factors are shown in a log−log plot as a function of the slope $\bar{\alpha}$. The vertical continuous lines represent the slope values for the PS5 and PMMA microbeads, and the vertical dashed line corresponds to $\bar{\alpha} = 1/2$, where the method exhibits the largest sensitivities. Figure 2b shows that there exists three sensitivity regimes (color-shaded areas) (i) $\bar{\alpha} < 1/4$ and $\bar{\alpha} > 1$, where $s_{\kappa p}^{c_f} > s_{\kappa p}^{\alpha}, s_{\kappa p}^{\rho_f}, s_{\kappa pp}^{\rho}$ and the relative error for the speed of sound ϵ_{c_f} dominates; (ii) $1/4 < \bar{\alpha} < 1/2$, where the relative error for the particle density $\epsilon_{\rho p}$ dominates; (iii) $1/2 < \bar{\alpha} < 1$, where the relative error in the slope ϵ_α dominates. For $\bar{\alpha} > 1/2$ the microparticle compressibility is negative, which is a feature of meta-materials in transition states.[35]

DOI: 10.1021/acs.analchem.7b01388
Anal. Chem. 2017, 89, 8917−8923

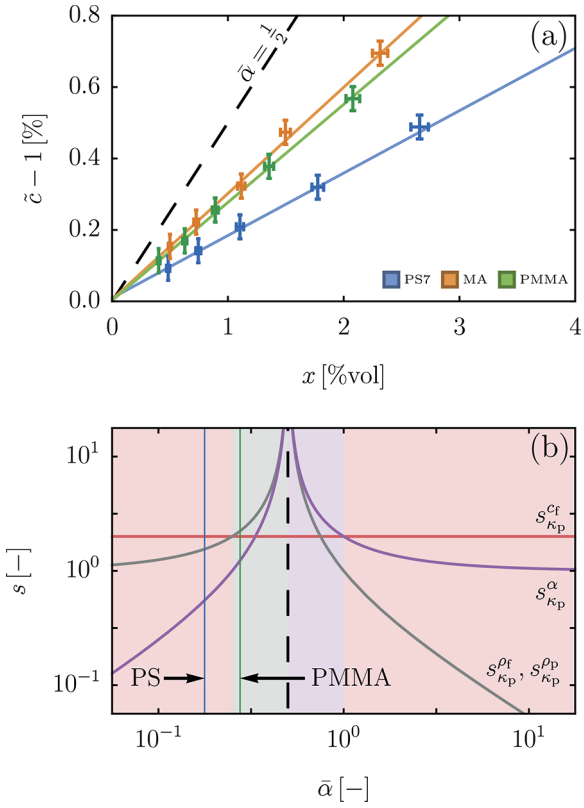

Figure 2. (a) Change in the relative speed of sound $\tilde{c} - 1$ [%] as a function of the particle volume fraction x [%] for polymer beads: PS 7 μm, MA and PMMA (error crosses). (b) Sensitivity factors eqs 10−12 for κ_p as a function of the average slope $\bar{\alpha}$. Vertical lines represent the slopes for PS7 (blue) and PMMA (green), and the reference $\bar{\alpha} = \frac{1}{2}$ (black dashed). The shaded areas represent the three regimes where the method is more sensitive to measurement of c_f(red), ρ_f, ρ_p (gray), and α (purple), respectively.

Concerning the specific results, we note that the PMMA data have been acquired under the worst operative conditions because of the small particle diameter $2a = 3$ μm. Nevertheless, fairly accurate results are obtained since the estimated errors for $\bar{\kappa}_p$ and $\bar{\rho}_p$ are small, $\epsilon_{\kappa p} = 3.4\%$, and $\epsilon_{\rho p} = 1.4\%$. Furthermore, we note that the measurements for PS5 microbeads should be affected more by the error on the microbead density compared to PS7 because of their smaller radius, see eq 18. However, the method performs in the regime $\alpha < 1/2$, in which the error for the microbead density is less important, and we achieved a better estimate of the compressibility based on a more accurate measurement of the slope $\bar{\alpha}$, since $s_{\kappa p}^{c_f}$ and σ_{c_f} are the same for PS5 and PS7.

Previously reported compressibility measurements[7,23,36,37] were based on assumed density and/or size values, and no error analysis was performed. By measuring the microparticle compressibility decoupled from the density with the proposed neutral-buoyant method, no assumptions regarding the value of the density needed to be made. The sensitivity analysis further proves the reliability and the robustness of the method with respect to the most critical experimental step, which is the microparticle density measurement by centrifugation and visual determination of the buoyancy criterion.

Acoustic Properties of Human Cells. Figure 3 shows the fitting of eq 5 to the data obtained from the speed of sound measurements of suspensions containing human cells (only nonfixed data are shown for visual clarity). Note that for these measurements the error crosses are larger than the cases of polymer particles, furthermore some of the data, e.g., RBC, show a systematic deviation from the linear interpolation. These effects are most likely due to the intrinsic biological variability of the biological samples.

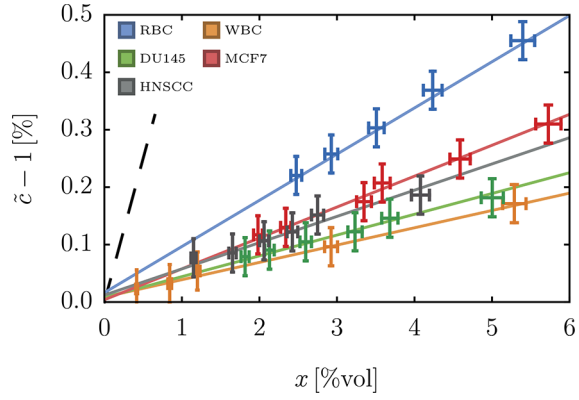

Figure 3. (a) Data points with error bars and regression lines for the change in the relative speed of sound $\tilde{c} - 1$ [%] as a function of the particle volume fraction x for human cells: RBC, WBC, DU-145, MCF-7, and LU-HNSCC-25. The dashed line is the reference slope $\bar{\alpha} = \frac{1}{2}$.

Table 2 lists the physical parameters for human cell lines extracted from the experiments reported in Figure 3. We observe that the slopes $\bar{\alpha}$ are between 2 and 10 times lower than those obtained for the microbeads and listed in Table 1. Therefore, the method works in a regime where the relative error in the speed of sound plays the most important role in the accuracy of the compressibility measurements. We note that for small values of the slope $\bar{\alpha}$, where relative error is large, eqs 10−12 lead to $s_{\kappa_f}^{\alpha} \to 0$ and $s_{\kappa_f}^{\rho_p} \to 1$, which stabilizes the error in the determination of the particle compressibility with respect to

Table 1. List of the Values for the Best Fit Slopes, Neutral Buoyant Solution Properties, Suspended Particle Properties, and Corresponding Reference Values for Polymer Particle Experiments[a]

	slope	physical parameters					reference values	
sample	$\bar{\alpha}$ [−]	$\bar{\rho}_f$ [kg/m^3]	$\bar{c}_f$ [m/s]	$\bar{\kappa}_f$ [TPa^{-1}]	$\bar{\rho}_p$ [kg/m^3]	$\bar{\kappa}_p$ [TPa^{-1}]	$\bar{\rho}_p$ [kg/m^3]	$\bar{\kappa}_p$ [TPa^{-1}]
PS5	0.177(1)	1058.5(1)	1493.2(5)	423.7(3)	1058(6)	273(2)	1050−1060	210−240[23,29]
PS7	0.175(3)	1059.6(1)	1493.1(5)	423.3(3)	1059(3)	276(3)	1050−1060	210−240[23,29]
MA	0.297(5)	1504.7(1)	1480.0(5)	303.4(2)	1500(1)	124(3)	1500−1510	∼90[13]
PMMA	0.274(2)	1185.7(1)	1485.8(5)	382.0(3)	1184(17)	173(6)	1190−1200	N. A.

[a]Polystyrene 5 μm (PS5), polystyrene 7 μm (PS7), melamine 10 μm (MA), and polymethylmethacrylate 3 μm (PMMA). The error on the last significant digit is in parentheses, 423.7(3) = 423.7 ± 0.3.

DOI: 10.1021/acs.analchem.7b01388
Anal. Chem. 2017, 89, 8917−8923

Table 2. List of the Values for the Best Fit Slopes α, Neutral Buoyant Solution Properties (Subscript f), Suspended Particle Properties (Subscript p), and Corresponding Reference Values for Human Cell Experiments[a]

	slope	physical parameters					reference values	
sample	$\bar{\alpha}$ [−]	$\bar{\rho}_f$ [kg/m^3]	$\bar{c}_f$ [m/s]	$\bar{\kappa}_f$ [TPa^{-1}]	$\bar{\rho}_p$ [kg/m^3]	$\bar{\kappa}_p$ [TPa^{-1}]	$\bar{\rho}_p$ [kg/m^3]	$\bar{\kappa}_p$ [TPa^{-1}]
RBC	0.080(2)	1102.9(1)	1510.2(5)	397.5(3)	1101(13)	334(2)	1100	330[27]
RBCfx	0.058(1)	1100.9(6)	1510.1(5)	398.3(3)	1091(14)	356(2)	N. A.	N. A.
WBC	0.030(1)	1055.7(1)	1506.4(5)	417.4(3)	1054(3)	393(1)	N. A.	N. A.
WBCfx	0.026(1)	1046.1(1)	1505.9(5)	421.5(3)	1045(3)	400(1)	1019	399[29]
DU-145	0.036(2)	1064.7(4)	1507.2(5)	413.5(3)	1062(1)	384(1)	N. A.	N. A.
DU-145fx	0.026(1)	1037.3(1)	1505.9(5)	425.1(3)	1036(1)	404(1)	1018	425[27]
MCF-7	0.054(1)	1056.6(1)	1507.0(5)	416.8(3)	1055(1)	373(1)	1068	380−422[23,38]
MCF-7fx	0.036(1)	1037.3(1)	1506.4(5)	424.8(3)	1035(1)	395(1)	N. A.	N. A.
LU-HNSCC-25	0.045(1)	1062.8(1)	1507.0(5)	414.3(3)	1061(1)	377(3)	N. A.	N. A.
LU-HNSCC-25fx	0.023(1)	1041.7(1)	1506.3(5)	423.1(3)	1040(1)	404(1)	N. A.	N. A.

[a]Red blood cells (RBC), white blood cells (WBC), prostate cancer cells (DU-145), breast cancer cells (MCF-7), and head and neck squamous cancer cells (LU-HNSCC-25). Suffix "fx" denote a fixed sample.

increasing relative errors for the smaller slope values. This stabilization is confirmed by data in Table 2, where for a broad range of slopes (e.g., $\bar{\alpha}^{RBC} = 0.080(2)$ and $\bar{\alpha}^{WBCf} = 0.026(1)$) the lower slopes feature relative errors larger than the steeper slopes, but the particle compressibility has almost the same accuracy. Note that the relative error for the compressibility that we found using our measurement method ϵ_{κ_f}(MCF-7) ≈ 2.7% is ∼3 times lower than that reported by,[38] which is ϵ_{κ_f}(MCF-7) ≈ 7.9%. We ascribe this reduction to the use of ensemble averaging versus single-particle measurements and the concurrent determination of density versus the use of a predetermined value as in ref 38. In regards to the physical parameters of nonfixed and fixed cell samples, we observe that fixation lowers the density and increases the compressibility.

Finally, Table 3 reports the scattering coefficients and the acoustophoretic contrast factors and their errors for the measured human cells in PBS ($\bar{\rho}_f$ = 1004. 00(1) kg/m^3 and $\bar{c}_f$ = 1508.2(5) m/s).

Table 3. Scattering Coefficients f_0 and f_1 and Acoustophoretic Contrast Factor Φ_0 for Cells in PBS[a]

sample	$\bar{f}_0$ [−]	$\bar{f}_1$ [−]	$\bar{\Phi}_0$ [−]
RBC	0.236(9)	0.060(5)	0.327(7)
RBCfx	0.188(9)	0.054(6)	0.270(8)
WBC	0.103(1)	0.033(1)	0.152(2)
WBCfx	0.086(2)	0.027(1)	0.126(2)
DU-145	0.122(3)	0.038(1)	0.178(3)
DU-145fx	0.077(3)	0.021(1)	0.109(3)
MCF-7	0.149(3)	0.032(1)	0.198(3)
MCF-7fx	0.098(1)	0.021(1)	0.129(1)
LU-HNSCC-25	0.139(7)	0.037(1)	0.194(7)
LU-HNSCC-25fx	0.078(1)	0.023(1)	0.113(2)

[a]Red blood cells (RBC), white blood cells (WBC), prostate cancer cells (DU-145), breast cancer cells (MCF-7), and head and neck squamous cancer cells (LU-HNSCC-25). Suffix "fx" denotes a fixed sample.

CONCLUSIONS

We have presented an experimental method that allows for the accurate determination of the density and compressibility of microbeads and cells. By a thorough error analysis we have provided quantitative expressions for the sensitivity factors for the acoustic parameters obtained by the method. The method was validated by measuring the acoustic parameters of reference polymer microbeads. Further, we have used the method to determine the acoustic parameters for the most common cell populations encountered in acoustophoretic applications. We have discussed the experimental errors in the light of the microparticle properties and demonstrated the robustness in determining the compressibility by speed-of-sound measurements under the neutral-buoyancy condition, where the explicit dependence of the density drops out. Specifically, we have identified three compressibility/slope-dependent regimes in the method sensitivity and a region $\bar{\alpha} \sim 1/2$ where the results can be affected by very large errors. Finally, we reconstructed the acoustophoretic contrast factor and the relative error for polymer beads in CsCl/water solutions and cells in PBS. The proposed method allows for a consistent and fairly accurate determination of the compressibility and density, and hence of the acoustic scattering coefficients, for cell populations.

These parameters are essential for predicting the feasibility of cell manipulation by acoustophoresis and for calculating optimal buffer conditions for maximum acoustophoretic discrimination between two cell types.

This method is of value in broader areas beyond the acoustofluidics' community, as various biomedical fields need a robust and reproducible method to determine the acoustic properties of different cell types to define the preconditions (e.g., calculating optimal buffer conditions) for performing successful and optimized cell separation based on acoustophoresis, for example, separation of WBC subpopulations (lymphocytes, monocytes, granulocytes), separation of RBCs from WBCs, circulating tumor cells (CTCs) from blood, and differentiated from undifferentiated stem cells, and more. The ability to optimize acoustophoretic separations will be useful for enhancing the enrichment and purification of cellular prognostic biomarkers, e.g., CTCs from blood containing RBCs and WBCs.

AUTHOR INFORMATION

Corresponding Authors

*E-mail: kevin.cushing@bme.lth.se.
*E-mail: fabio.garofalo@bme.lth.se.

ORCID

Kevin W. Cushing: 0000-0002-0533-9906
Cecilia Magnusson: 0000-0002-0186-7736

DOI: 10.1021/acs.analchem.7b01388
Anal. Chem. 2017, 89, 8917−8923

Author Contributions

[⊥]K.W.C. and F.G. contributed equally to this work.

Notes

The authors declare no competing financial interest.

■ ACKNOWLEDGMENTS

This work was supported by the Knut and Alice Wallenberg Foundation (Grant No. KAW 2012.0023).

■ REFERENCES

(1) Nordin, M.; Laurell, T. *Lab Chip* **2012**, *12*, 4610−4616.
(2) Evander, M.; Nilsson, J. *Lab Chip* **2012**, *12*, 4667−4676.
(3) Augustsson, P.; Laurell, T. *Lab Chip* **2012**, *12*, 1742−1752.
(4) Manneberg, O.; Svennebring, J.; Hertz, H. M.; Wiklund, M. *J. Micromech. Microeng.* **2008**, *18*, 095025.
(5) Augustsson, P.; Magnusson, C.; Nordin, M.; Lilja, H.; Laurell, T. *Anal. Chem.* **2012**, *84*, 7954−7962.
(6) Ding, X.; Peng, Z.; Lin, S.-C. S.; Geri, M.; Li, S.; Li, P.; Chen, Y.; Dao, M.; Suresh, S.; Huang, T. J. *Proc. Natl. Acad. Sci. U. S. A.* **2014**, *111*, 12992−12997.
(7) Petersson, F.; Åberg, L.; Sward-Nilsson, A. M.; Laurell, T. *Anal. Chem.* **2007**, *79*, 5117−23.
(8) Titushkin, I.; Cho, M. *Biophys. J.* **2006**, *90*, 2582−2591.
(9) Cross, S.; Jin, Y.-S.; Rao, J.; Gimzewski, J. K. *Nat. Nanotechnol.* **2007**, *2*, 780−783.
(10) Dao, M.; Lim, C.; Suresh, S. *J. Mech. Phys. Solids* **2003**, *51*, 2259−2280.
(11) Li, Q. S.; Lee, G. Y. H.; Ong, C. N.; Lim, C. T. *Biochem. Biophys. Res. Commun.* **2008**, *374*, 609−613.
(12) Remmerbach, T.; Wottawah, F.; Dietrich, J.; Lincoln, B.; Wittekind, C.; Guck, J. *Cancer Res.* **2009**, *69*, 1728.
(13) Settnes, M.; Bruus, H. *Phys. Rev. E* **2012**, *85*, 016327.
(14) Radmacher, M.; Fritz, M.; Kacher, C.; Cleveland, J.; Hansma, P. *Biophys. J.* **1996**, *70*, 556−567.
(15) Addae-Mensah, K. A.; Wikswo, J. P. *Exp. Biol. Med.* **2008**, *233*, 792−809.
(16) Chien, S.; Sung, K.; Skalak, R.; Usami, S.; Tozeren, A. *Biophys. J.* **1978**, *24*, 463−487.
(17) Schmid-Schönbein, G.; Sung, K.; Tözeren, H.; Skalak, R.; Chien, S. *Biophys. J.* **1981**, *36*, 243−256.
(18) Ziemann, F.; Rädler, J.; Sackmann, E. *Biophys. J.* **1994**, *66*, 2210−2216.
(19) Hénon, S.; Lenormand, G.; Richert, A.; Gallet, F. *Biophys. J.* **1999**, *76*, 1145−1151.
(20) Zhang, H.; Liu, K.-K. *J. R. Soc., Interface* **2008**, *5*, 671−690.
(21) Gossett, D. R.; Tse, H. T. K.; Lee, S. A.; Ying, Y.; Lindgren, A. G.; Yang, O. O.; Rao, J.; Clark, A. T.; Carlo, D. D. *Proc. Natl. Acad. Sci. U. S. A.* **2012**, *109*, 7630−7635.
(22) Otto, O.; et al. *Nat. Methods* **2015**, *12*, 199−202.
(23) Hartono, D.; Liu, Y.; Tan, P. L.; Then, X. Y. S.; Yung, L.-Y. L.; Lim, K.-M. *Lab Chip* **2011**, *11*, 4072.
(24) Shields, C. W.; Sun, D.; Johnson, K. A.; Duval, K. A.; Rodriguez, A. V.; Gao, L.; Dayton, P. A.; López, G. P. *Angew. Chem., Int. Ed.* **2014**, *53*, 8070−8073.
(25) Mott, P. H.; Dorgan, J. R.; Roland, C. M. *J. Sound Vibr.* **2008**, *312*, 572−575.
(26) Wood, A. B.; Lindsay, R. B. *A Textbook of Sound*; AIP Publishing, 1956; Vol. *9*; pp 37−37.
(27) Dukhin, A. S.; Goetz, P. J.; van de Ven, T. G. *Colloids Surf., B* **2006**, *53*, 121−126.
(28) Barrett-Gueltepe, M. A.; Gueltepe, M. E.; Yeager, E. B. *J. Phys. Chem.* **1983**, *87*, 1039−1045.
(29) Barnkob, R.; Augustsson, P.; Magnusson, C.; Lilja, H.; Laurell, T.; Bruus, H. *Proceedings of the 15th MicroTAS*, Seattle, WA, October 2−6, 2011; pp 127−129.
(30) Barnkob, R.; Iranmanesh, I.; Wiklund, M.; Bruus, H. *Lab Chip* **2012**, *12*, 2337−2344.
(31) *Antoon-Paar DSA 5000M*, http://www.anton-paar.com/, 2015.
(32) Krystek, M.; Anton, M. *Meas. Sci. Technol.* **2008**, *19*, 079801.
(33) Haynes, W. *CRC Handbook of Chemistry and Physics*, 94th ed.; CRC Press, 2013.
(34) Muller, P. B.; Bruus, H. *Phys. Rev. E* **2014**, *90*, 043016.
(35) Nicolaou, Z. G.; Motter, A. E. *Nat. Mater.* **2012**, *11*, 608−613.
(36) Hirawa, S.; Masudo, T.; Okada, T. *Anal. Chem.* **2007**, *79*, 3003.
(37) Settnes, M.; Bruus, H. *Proceedings of the 15th MicroTAS*, Seattle, WA, October 2−6, 2011; pp 160−162.
(38) Yang, T.; Bragheri, F.; Nava, G.; Chiodi, I.; Mondello, C.; Osellame, R.; Berg-Sørensen, K.; Cristiani, I.; Minzioni, P. *Sci. Rep.* **2016**, *6*, 23946.

■ NOTE ADDED AFTER ASAP PUBLICATION

This paper was originally published ASAP on August 15, 2017. Due to a production error, the π was missing in eq 3. The corrected version was reposted on August 21, 2017.

DOI: 10.1021/acs.analchem.7b01388
Anal. Chem. 2017, 89, 8917−8923